

Strong Ground Motion Attenuation Relations for Chilean Subduction Zone Interface Earthquakes

V. Contreras & R. Boroschek

Department of Civil Engineering, University of Chile, Chile



SUMMARY:

Attenuation formulas are established for horizontal Peak Ground Accelerations (PGA) and horizontal Spectral Accelerations (SA) using a database of Chilean seismic records. This is the first Chilean study that includes the development of a spectral acceleration attenuation model. The database used corresponds to records of earthquakes from the Nazca plate and the South American plate interface (thrust-faulting) that occurred between 1985 and 2010. We have included accelerograms from the 2010 Mw 8.8 Maule Chile earthquake, one of the largest strong motion recordings world-wide. The earthquake database analyzed enabled a first estimation of spectral acceleration attenuation relations for Chilean interface earthquakes. The proposed formulas take into account differences in the soil type (rock or soil) according to the Chilean code soil classification. These ground motion prediction equations could be useful to improve the seismic hazard assessment in Chile and others similar subduction zones.

Keywords: Maule Chile earthquake, attenuation, subduction zone, ground motion prediction

1. INTRODUCTION

Chile is located in one of the most seismically active regions on the planet. The occurrence of earthquakes in Chilean territory is mainly explained by the subduction process of the Nazca plate beneath the South American plate, which occurs with a convergence rate of about 8 cm/yr. This tectonic process is responsible for the uplift of the Andes Mountains and for the active volcanism present in the country. Most of the large earthquakes, Magnitude 8 or greater, have occurred on the interface between both plates, including the largest instrumentally recorded earthquake in the world: the 1960 Mw 9.5 earthquake in southern Chile. In this context, the development of attenuation relations for the earthquakes that occurs in this specific subduction zone is an important input in the seismic hazard assessment of Chile, and eventually for similar tectonic zones.

In this paper we present attenuation formulas for horizontal Peak Ground Accelerations (PGA) and horizontal Spectral Accelerations (SA) for subduction interface earthquakes recording in the Chilean territory. Attenuation curves were estimated using the maximum likelihood regression method. The proposed formulas take into account differences in the soil type according to the Chilean code soil classification. We briefly compare the obtained results with the accelerations from existing prediction equations for subduction zones.

2. STRONG MOTION DATABASE

The database used in this study contains accelerograms recorded in the Chilean territory during interface (thrust-faulting) earthquakes occurred between 1985 and 2010, including the accelerograms from the recent 2010 Mw 8.8 Maule Chile earthquake. The database was generated from public accelerographic data and accelerograms recorded by the University of Chile (UCh).

The University of Chile has maintained strong motion arrays in operation since the mid-1960, controlled by the National Accelerograph Network at the Department of Civil Engineering (RENADIC) and the Seismological Service at the Department of Geophysics (GUC). Most of the instruments are analogue accelerometers (SMA-1 or similar) located inside one story buildings.

We used a subset of the overall database compiled considering only the interface events with Magnitude $M_w \geq 6.5$. The resulting subset consists in 117 accelerograms from 13 interface earthquakes recorded at 79 stations, and located at distances between 30 and 600 km. The earthquakes used in this study, listed in Table 2.1., correspond to 9 main events and 4 aftershocks with large magnitudes.

Moment Magnitude (M_w) was obtained from the Harvard Centroid Moment Tensor (CMT) catalogue. The M_w 8.8 Chile earthquake, occurred on February 27, 2010 in the south central Chilean region of Maule is the largest magnitude earthquake included in the database.

The date, time, location of the epicenters (Lat, Long) and focal depth (H) were taken from the Seismologic Service of the UCh. The epicenters of earthquakes and location of the recording stations are shown in Fig. 2.1. (in this Figure the earthquakes are listed as indicated in Table 2.1.). Despite the small dataset, this is an initial attempt to capture the general behaviour of spectral accelerations at different periods for the country. This is necessary because of the known regional differences in seismicity and attenuation characteristics of the South America interplate region.

Due to the limited number of accelerograms used in this study, we decided to classify the sites of the recording stations only into two generic groups: Rock and Soil. Based on different type of geotechnical information we classify the sites according to the Chilean code soil classification, considering that the sites located on Rock comply with $V_{S30} \geq 900$ m/s (average shear wave velocity over 30 m), or $RQD \geq 50\%$ (Rock Quality Designation according to ASTM D 6032), or $q_u \geq 10$ MPa (Compressive Strength). In other cases we classify the sites as Soil.

Table 2.1. List of interface earthquakes used to develop attenuation relations

#	Date (dd-mm-yy)	UTC Time (hh:mm)	M_w	Lat. S	Long. W	H (km)	Number of Records	
							Rock	Soil
1	03-03-1985	22:46	7.9	-33.24	-71.85	33	5	22
2	03-03-1985 ^(a)	23:38	7.3	-32.74	-71.21	33	1	2
3	09-04-1985 ^(a)	01:56	7.1	-34.13	-71.62	38	1	9
4	30-07-1995	05:11	8.0	-23.57	-70.60	33	1	1
5	30-01-1998	12:16	7.0	-23.51	-69.83	44	1	0
6	23-06-2001	20:33	8.4	-16.26	-73.64	33	1	6
7	07-07-2001 ^(b)	09:38	7.6	-17.40	-71.80	37	0	1
8	18-04-2002	16:08	6.6	-27.51	-70.09	53	1	0
9	20-06-2003	13:30	6.8	-30.65	-71.81	24	0	1
10	30-04-2006	21:40	6.5	-26.84	-71.15	18	0	2
11	14-11-2007	15:40	7.7	-22.69	-70.22	39	6	11
12	16-12-2007 ^(c)	08:09	6.7	-22.95	-70.18	42	5	9
13	27-02-2010	06:34	8.8	-36.29	-73.24	30	3	28

(a) Aftershocks of the 03-03-1985 (22:46) earthquake.

(b) Aftershock of the 23-06-2001 earthquake.

(c) Aftershock of the 14-11-2007 earthquake.

Focal mechanisms were obtained from published works and from the CMT solutions. This information was subsequently revised considering the proximity of the events to the subduction zone interface and the alignment of the mechanisms with the dip of the interface. The closest distance to the rupture surface (R_{rup}) is used as source to site distance. To estimate this parameter we modeled the earthquakes

fault plane using the CMT solutions and the aftershocks distributions, considering that normally the rupture area is smaller than aftershocks area. For main events without a defined aftershock rupture area (events 5 and 8) and for aftershocks of the 03-03-1985 earthquake (events 2 and 3) we used hypocentral distance instead of R_{rup} .

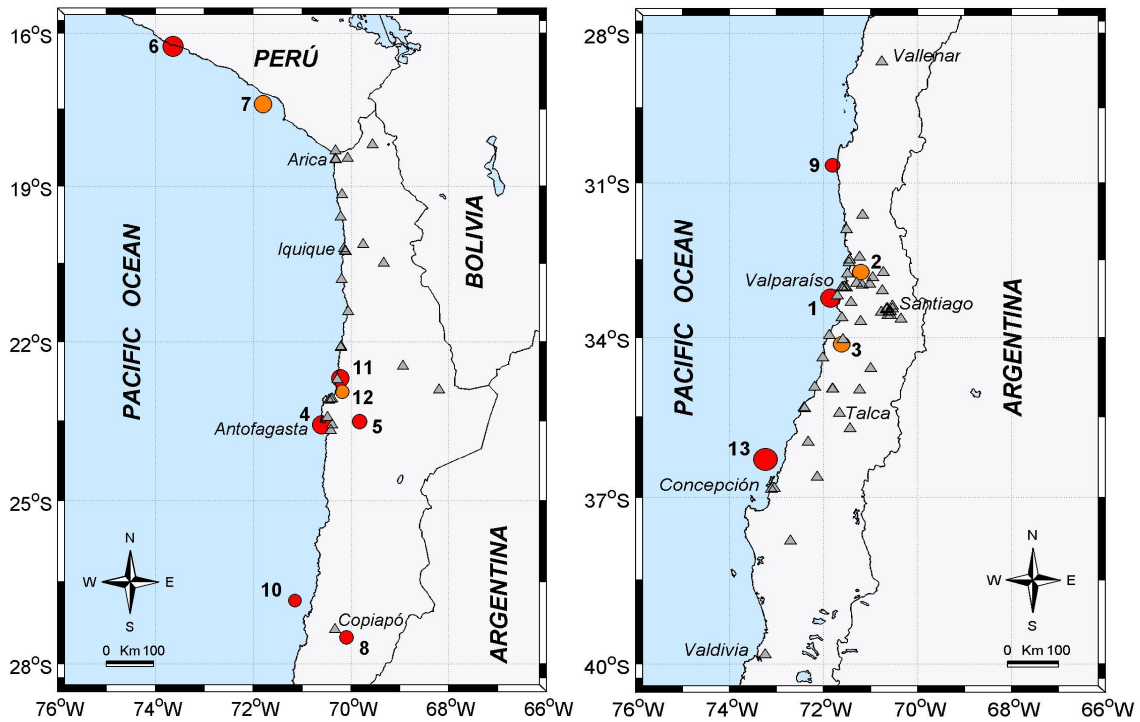


Figure 2.1. Map of north and central Chile showing epicenters (listed circles) of earthquakes used in this study. Red circles correspond to main events and orange circles correspond to aftershocks. The circles size is proportional to the Magnitud. Grey triangles represent the strong motion stations.

The magnitude-distance distribution of the database used is shown in the Fig. 2.2., splitting the data according to the soil type. The data from the Mw 8.8 2010 earthquake has a strong influence on the development of ground motion prediction equations presented in this study, introducing new data for large magnitudes and short source distances.

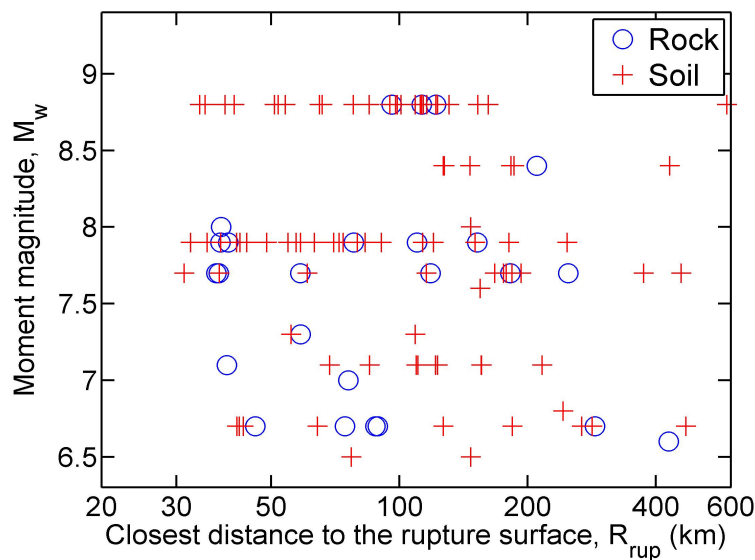


Figure 2.2. Distribution of the data for interface earthquakes used in this study.

2.1. Data processing procedure

The procedure used for record processing is similar to techniques described in the literature for high-cut filtering (Akkar et al. 2011) and for low-cut filtering (Akkar and Bommer 2006 and Paolucci et al. 2008). Recordings were digitized and processed in order to preserving high and low frequency signal to the maximum possible. The Fourier Amplitude Spectrum (FAS) was inspected in log-log space to identify the maximum usable frequency (f_{max}) and to preliminarily estimate the low-cut filter corner (f_{min}). Typically, f_{max} was taken as 90 Hz for a Nyquist frequency of 100 Hz and 40 Hz for a Nyquist frequency of 50 Hz. An iterative process was performed to select the final value of f_{min} , in which the value was varied up and down and the integrated displacement histories and displacement response spectra were inspected.

This process is illustrated in Fig. 2.3. for the VINA record from the Mw 8.8 2010 earthquake. We seek the lowest value of f_{min} that preserves a natural appearance to the record in the time domain without obvious drift from low frequency noise. For the VINA record (NS component), f_{min} was selected as 0.03 Hz. Filtering was applied in the time domain using an acausal fourth order Butterworth filter. Finally, pseudo acceleration response spectra at 5% damping were calculated for a period band ending slightly short of $1/f_{min}$. More details about record processing can be found in Boroschek et al. 2012.

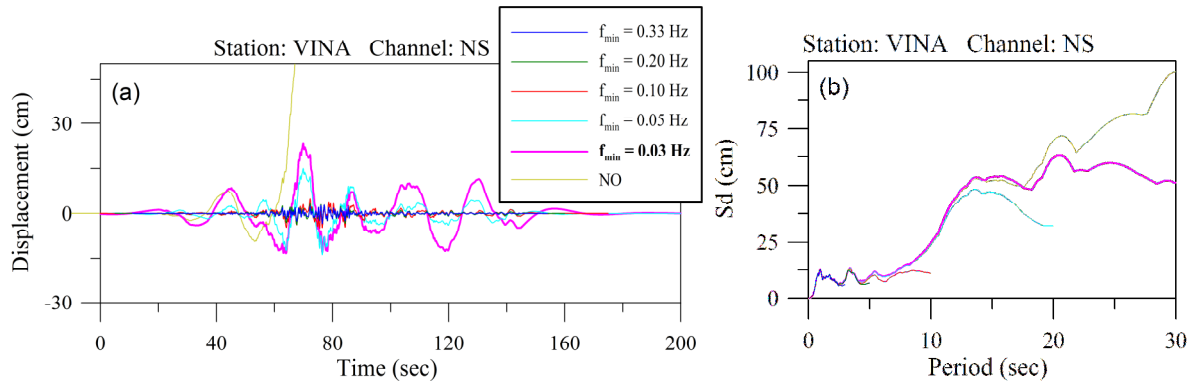


Figure 2.3. Sensitivity of integrated displacements and displacement response spectra to different low-cut filter corners. The case indicated with 'NO' corresponds to direct integration of the VINA record.

A significant portion of the database corresponds to accelerograms recorded with analogue instruments for which the mentioned processing was difficult to apply, limiting the information for long periods. For this reason, we presented the predictions equations for periods up to 2 seconds, although we calculated spectral accelerations for higher periods for several records.

3. REGRESSION METHOD AND FUNCTIONAL FORM

Regression of the database was performed using the one-stage maximum likelihood regression method. We used the following simple functional form:

$$\log_{10}(Y) = C_1 + C_2 M_w + C_3 H + C_4 R - g \log_{10}(R) + C_5 Z \quad (3.1)$$

where Y is either Peak Ground Acceleration (PGA) or 5% damped Spectral Acceleration (SA). In both cases the geometric mean of two horizontal components in units of g was used. M is the moment magnitude, H is the focal depth in kilometers, $R = \sqrt{R_{rup}^2 + \Delta^2}$ with R_{rup} the closest distance to the rupture surface in kilometers and Δ a near-source saturation term, given by $\Delta = C_6 10^{C_7 M_w}$. $g = C_8 + C_9 M_w$ is the geometrical spreading coefficient. For Rock sites $Z = 0$ and for Soil sites $Z = 1$. Coefficients C_i , with $i = 1, \dots, 9$, were determined by regression analysis.

The coefficients C_6 and C_7 (associated to the near-source saturation term) and the coefficients C_8 and C_9 (associated to the geometrical spreading coefficient) were calculated using an optimization algorithm that allowed minimize the mean of residuals for the PGA data with distances lesser than or equal to 80 km. This subset of the data, consisting in 47 recordings, was selected considering the distance range where the possible saturation occurs. These coefficients were fixed for all periods analyzed. The coefficients C_1 , C_2 , C_3 , C_4 and C_5 were calculated using the one-stage maximum likelihood regression method for each period; therefore the values of these coefficients vary with the period.

4. RESULTS OF THE REGRESSION

The regression coefficients dependent of period and standard deviation of the residuals (σ) are presented in the Table 4.1. Also, the variations of these parameters in function of period are shown in Fig. 4.1. As found in previous work, there is a weak depth effect given by the coefficient C_3 , with deeper events causing larger accelerations. According to Fig. 4.1 this effect increases with period. Inspection of the coefficients C_5 shows that Soil accelerations exceed Rock accelerations by a factor ranging from 1.6 to 2. There is a tendency to higher amplifications for short periods in accordance to what is shown in Fig. 4.1. Standard deviations of the residuals are in the range of 0.21 to 0.26.

Table 4.1. Regression coefficients dependent of period and standard deviations of the residuals

Period (sec)	C_1	C_2	C_3	C_4	C_5	σ
PGA	-1.8559	0.2549	0.0111	-0.0013	0.3061	0.2137
0.04	-1.7342	0.2567	0.0111	-0.0016	0.2865	0.2311
0.10	-1.4240	0.2597	0.0081	-0.0019	0.2766	0.2557
0.15	-1.1244	0.2373	0.0062	-0.0017	0.2811	0.2594
0.20	-1.0028	0.2375	0.0023	-0.0014	0.2699	0.2469
0.25	-1.0232	0.2405	0.0014	-0.0011	0.2690	0.2349
0.30	-1.2836	0.2519	0.0044	-0.0009	0.2977	0.2434
0.35	-1.2239	0.2430	0.0031	-0.0007	0.3097	0.2495
0.40	-1.4161	0.2568	0.0049	-0.0008	0.3150	0.2414
0.45	-1.8610	0.2943	0.0084	-0.0008	0.3093	0.2322
0.50	-2.1228	0.3208	0.0094	-0.0008	0.2834	0.2272
0.60	-2.7134	0.3668	0.0141	-0.0008	0.2824	0.2174
0.70	-2.9001	0.3795	0.0152	-0.0009	0.2969	0.2221
0.80	-3.0909	0.4005	0.0147	-0.0009	0.2834	0.2279
0.90	-3.1439	0.3952	0.0163	-0.0010	0.2730	0.2260
1.00	-3.3352	0.4013	0.0186	-0.0010	0.2839	0.2351
1.10	-3.5092	0.4093	0.0202	-0.0011	0.2849	0.2379
1.20	-3.5599	0.4079	0.0211	-0.0011	0.2700	0.2374
1.30	-3.6365	0.4090	0.0218	-0.0010	0.2631	0.2429
1.40	-3.7061	0.4096	0.0225	-0.0010	0.2555	0.2425
1.50	-3.7750	0.4089	0.0228	-0.0010	0.2528	0.2459
1.60	-3.7924	0.4047	0.0226	-0.0009	0.2406	0.2483
1.70	-3.8670	0.4045	0.0234	-0.0008	0.2355	0.2498
2.00	-3.9051	0.4079	0.0215	-0.0008	0.2057	0.2592

The coefficients associated to the near-source saturation term were fixed for all periods as $C_6 = 0.0734$ and $C_7 = 0.3552$. The coefficients associated to the geometrical spreading term were fixed for all periods as $C_8 = 1.5149$ and $C_9 = -0.103$.

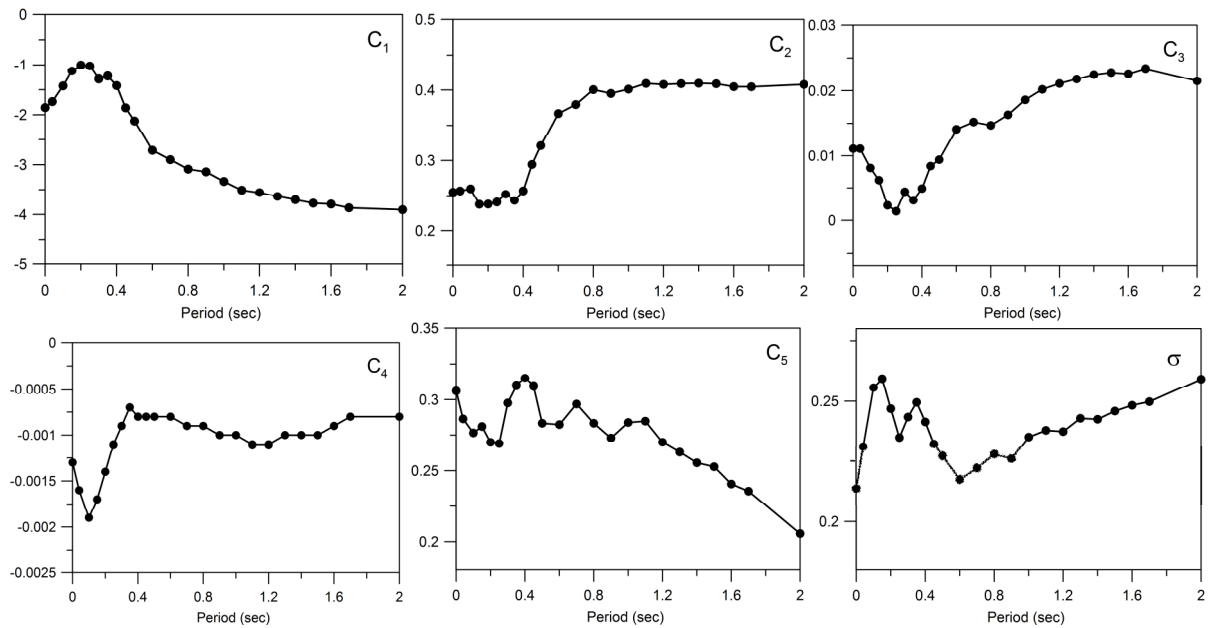


Figure 4.1. Variation of regression coefficients and standard deviation of residuals in function of period.

Fig. 4.2. shows for 0.04 and 1.0 seconds reference period the predicted spectral accelerations versus rupture distance for different magnitudes and soil conditions. It is clearly observed the effect of the saturation term for large magnitudes and near to fault distances. Considering for example an interface earthquake with Magnitude $M_w=8.5$ and focal depth $H=30\text{km}$, the developed relations predict spectral accelerations of 0.3g for Rock and 0.5g for Soil, for a period of 0.04 seconds; and 0.2g for Rock and 0.4g for Soil, for a period of 1.0 second.

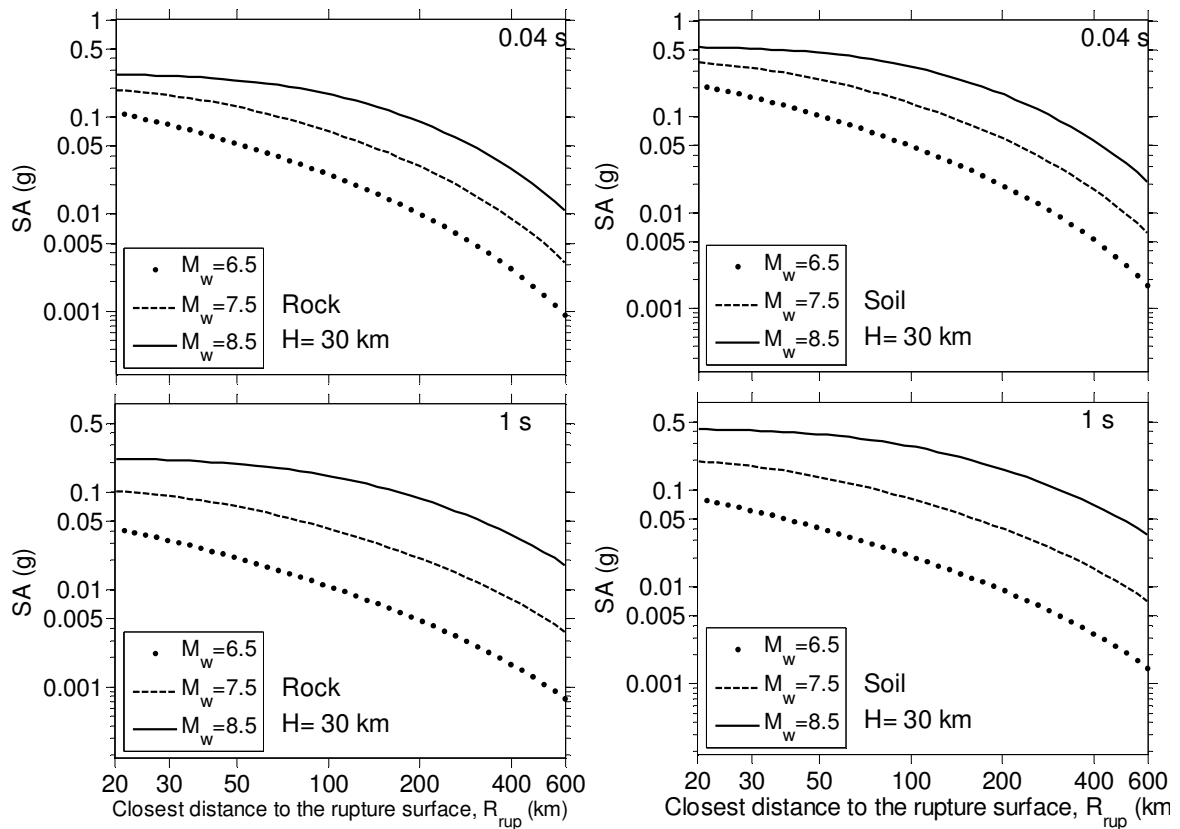


Figure 4.2. Attenuation curves obtained plotted for different magnitudes.

Relatively recent GMPEs for interface subduction zone were developed by Atkinson and Boore 2003, 2008 and Zhao et al. 2006, which we referred to subsequently as AB03 and ZEA06. The AB03 interface model was derived exclusively from subduction zone interface earthquakes. In contrast, the ZEA06 model constrains near fault ground motions from crustal and slab earthquakes. In Fig. 4.3. we compare predicted and observed accelerations for PGA, 0.4, 1.0 and 2.0 s, considering an earthquake with $M_w=8.8$ and $H=30$ km. Predicted curves proposed in this study for Rock and Soil are plotted. Also AB03 and ZEA06 models are plotted for the C/D boundary by averaging predictions for the two site classes. It is observed that the relations obtained present a good fit for the earthquake data plotted ($M_w=8.8\pm 0.5$). AB03 GMPE under-predicts the acceleration level, but it is consistent with the variation of data with distance (excepting 2.0 s data). The ZEA06 GMPE over-predicts the attenuation rate.

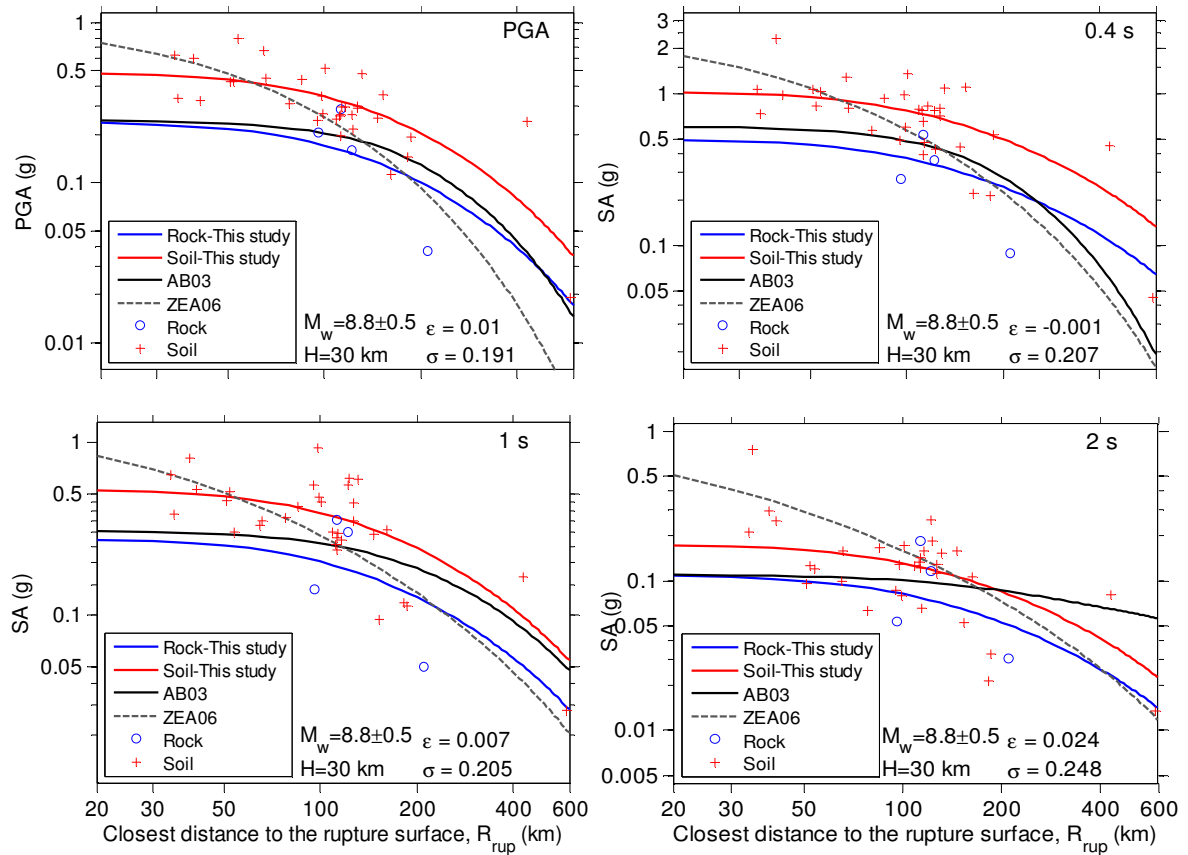


Figure 4.3. Comparison between predicted and observed accelerations ($M_w=8.8\pm 0.5$, $H=30$ km). The mean of residuals (ϵ) and the standard deviation of residuals (σ) for the data shown are indicated.

Fig. 4.4. shows the residuals of the regression as a function of source distance for PGA, 0.04, 0.2, 0.4, 1.0 and 2.0 seconds reference period. The residual is measured in log base 10 units and is defined as the difference between the log of the observed value and the log of the predicted value. Positive residual denotes underprediction and negative residual denotes overprediction. It is observed that the mean of residuals are near zero.

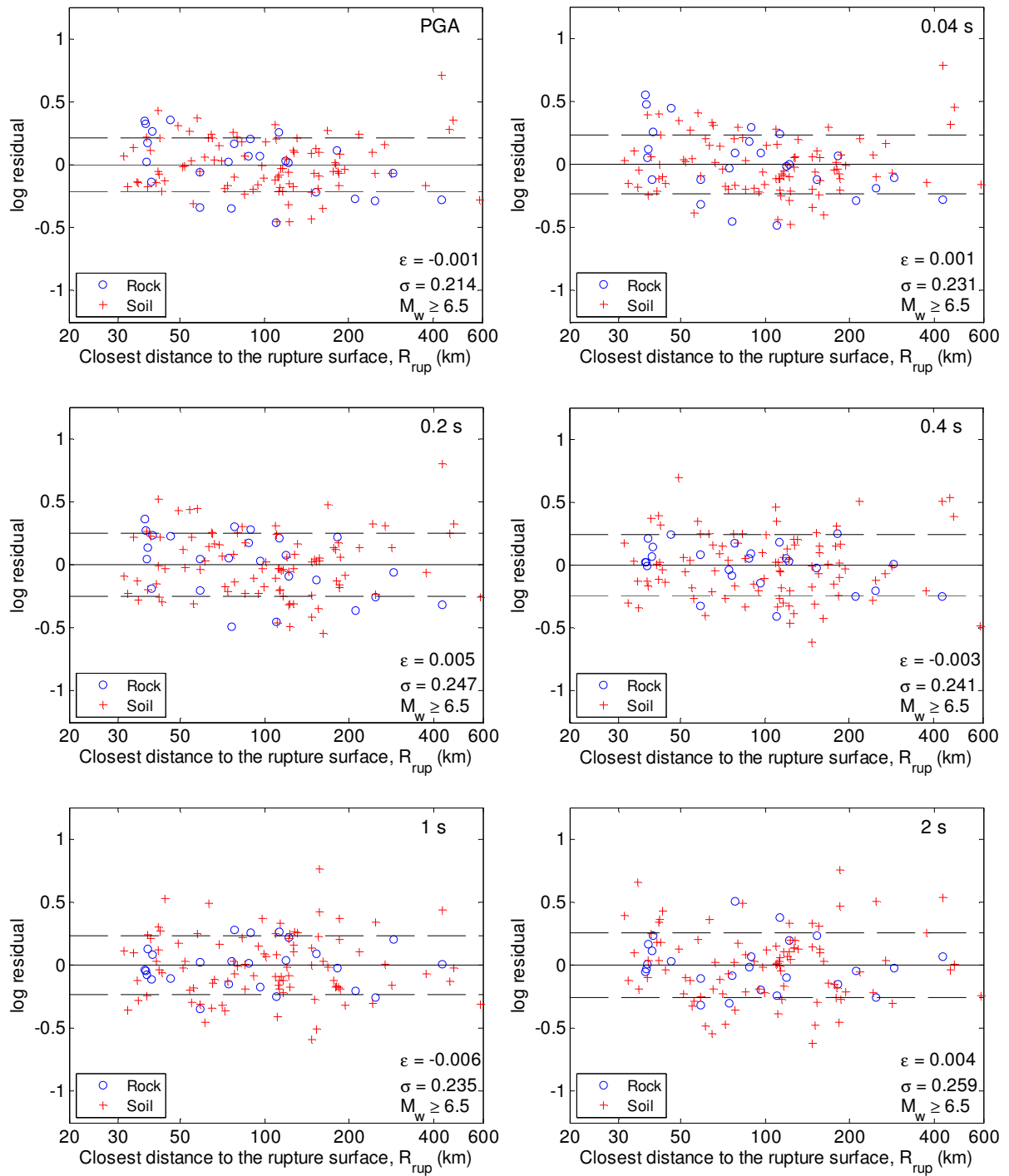


Figure 4.4. Log residuals (= log observed value – log predicted value) of the regression. The mean of residuals (ϵ) and the standard deviation of residuals (σ) for the entire database are indicated. Discontinuous lines represent one standard deviation.

Fig. 4.5. shows a comparison of observed response spectra versus predicted response spectra for some representative records. The relations proposed in this study, generally result in higher accelerations than those estimated in other works, with the exception of the ZEA06 model for near fault distances.

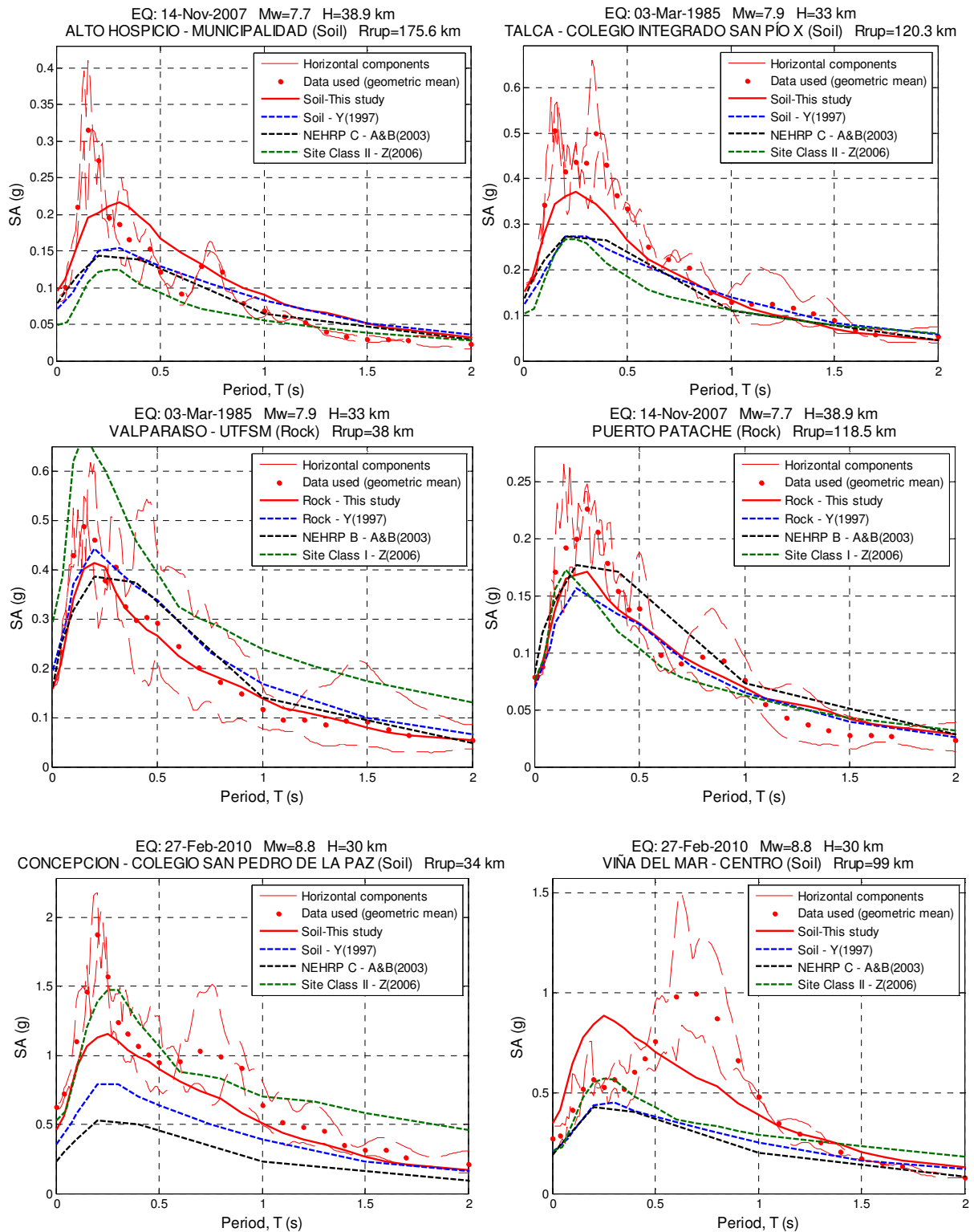


Figure 4.5. Comparison of observed response spectra versus predicted response spectra.

5. CONCLUSIONS

Accelerograms database was generated from public accelerographic data and data recorded by the University of Chile. For this work only data from Chilean interplate earthquakes was used in order to compare the results with relations from other seismic zones of the world, due to Chilean earthquake

events have been recognized before that they are underestimated by existing GMPE's. The earthquake database analyzed enabled a gross estimation of attenuation relations for Chilean interface earthquakes. These GMPEs could be useful to improve the seismic hazard assessment in Chile and others similar subduction zones. In particular, the relations obtained present a good fit for earthquakes with larger magnitudes, and the logarithmic standard deviations of the errors are in the range 0.21 to 0.26. The derived relations indicate that the accelerations at stations located in Soil are higher than those estimated at stations located on Rock by a factor of up to 2. For the Chilean case, the horizontal accelerations are generally higher than those estimated in studies where records from different subduction zones around the world are mixed. This issue highlights the need to develop GMPE's for specific subduction zones.

ACKNOWLEDGEMENT

The financial and technical support of the Civil Engineering Department of University of Chile and the effort of Engineer Pedro Soto installing and maintaining the instruments are gratefully acknowledged.

REFERENCES

- Akkar S. and Bommer J. J. (2006). Influence of long-period filter cut-off on elastic spectral displacements, *Earthquake Engineering & Structural Dynamics* **35**, 1145–1165.
- Akkar S., Kale Ö., Yenier E. and Bommer J. J. (2011). The high-frequency limit of usable response spectral ordinates from filtered analogue and digital strong-motion accelerograms, *Earthquake Engineering & Structural Dynamics* **40**, 1387–1401.
- Arango M. C., Strasser F. O., Bommer J. J., Boroschek R., Comte D. and Tavera H. (2010). A strong-motion database from the Peru–Chile subduction zone, *J. Seismology*, **15**, 19–41.
- Atkinson G. M. and Boore D. M. (2003). Empirical Ground-Motion Relations for Subduction-Zone Earthquakes and Their Application to Cascadia and Other Regions, *Bulletin of the Seismological Society of America*, **Vol. 93**, N° 4, pp. 1703-1729, August.
- Atkinson G. M. and Boore D. M. (2008). Erratum to Empirical Ground-Motion Relations for Subduction-Zone Earthquakes and Their Application to Cascadia and Other Regions, *Bulletin of the Seismological Society of America*, **Vol. 98**, N° 5, pp. 2567-2569, October.
- Boroschek R., Contreras V., Youp D. and Stewart J. (2012). Strong Ground Motion Attributes of the 2010 Mw 8.8 Maule Chile Earthquake, *Earthquake Spectra*. Accepted for publication.
- Delouis B., Nocquet J-M and Vallée M. (2010). Slip distribution of the February 27, 2010 Mw=8.8 Maule Earthquake, central Chile, from static and high-rate GPS, InSAR, and broadband teleseismic data, *Geophys. Res. Ltrs*, **37**, L17305.
- Kataoka S. (2011). Microtremor exploration at seven strong motion stations in Chile, *4th IASPEI/IAEE International Symposium: Effects of Surface Geology on Seismic Motion*, August 23-26, University of California Santa Barbara.
- Paolucci R., Rovelli A., Faccioli E., Cauzzi C., Finazzi D., Vanini M., Di Alessandro C., Calderoni G. (2008). On the reliability of long period spectral ordinates from digital accelerograms, *Earthquake Engineering & Structural Dynamics* **37**, 697–710.
- Youngs, R.R., S.-J. Chiou, W.J. Silva, and J.R. Humphrey (1997). Strong ground motion attenuation relationships for subduction zone earthquakes, *Seismol. Res. Let.* **68**, N°1, pp. 58–73, Jan./Febr.
- Zhao J. X., Zhang J., Asano A., Ohno Y., Oouchi T., Takahashi T., Ogawa H., Irikura K., Thio H. K., Somerville P. G., Fukushima Y. and Fukushima Y. (2006). Attenuation relations of strong ground motion in Japan using site classification based on predominant period, *Bull. Seis. Soc. Am.* **96** 898-913.